J. Am. Ceram. Soc., 95 [11] 3455–3462 (2012)
DOI: 10.1111/j.1551-2916.2012.05417.x

journal

Aqueous Route Synthesis of Mesoporous ZrO_2 by Agarose Templation

Xing Ma,[‡] Luke Klosterman,[‡] Yan-Yan Hu,[§] Xunpei Liu,[¶] Klaus Schmidt-Rohr,[§] Surya Mallapragada,[¶] and Mufit Akinc[‡,†]

[‡]Ames Laboratory and Department of Materials Science & Engineering, Iowa State University, Ames, Iowa 50011

[§]Ames Laboratory and Department of Chemistry, Iowa State University, Ames, Iowa 50011

[¶]Ames Laboratory and Department of Chemical and Biological Engineering, Iowa State University, Ames, Iowa 50011

Mesoporous zirconia with high surface area has been synthesized using self-assembling agarose gel as a template. Agarose gel was formed in the presence of aqueous zirconyl nitrate solutions followed by precipitation of zirconium (hydr)oxide in the gel framework. A porous zirconia structure is obtained by pyrolysis of agarose. Fourier transform infrared spectroscopy is employed to assess the agarose-zirconia precursor interaction. Changes in the C–O absorption bands indicate zirconium association with the OH groups of the agarose. Solid state ^{13}C NMR studies of the nanocomposite showed a shift in intensity from 70 to 75 ppm indicating conversion of ~7% of C–O–H to C–O–Zr. Scanning electron microscopy reveals that both agarose/zirconia nanocomposite and zirconia have similar morphological features as that of pure agarose gel confirming agarose templation. Phase transformation of zirconia from amorphous to tetragonal between 300°C and 500°C, and gradually into monoclinic phase up to 900°C is observed using X-ray powder diffraction. Specific surface area and pore size distribution are determined using nitrogen adsorption, employing BET and Barrett–Joyner–Halenda methods, respectively. The specific surface area of porous zirconia after heat treatment at 500°C was determined to be 86 m^2/g, which reduced with increasing temperature to 13 m^2/g above 900°C. Transmission electron microscopy confirmed the hierarchical structure of porous zirconia.

I. Introduction

Fabrication of porous materials has been an active topic of interest for a long time due to their special properties brought by the high surface area afforded by these materials.[1–3] Especially, porous metal oxides possess many advantages in industrial applications, such as drug delivery, catalysis, electrochemical sensing, and separation technologies. Among them, porous zirconia is of great interest for its thermal barrier, catalytic, and biosensor applications.[4,5] Due to its excellent biological properties,[6] porous zirconia exhibits great potential in biological application, such as enzyme immobilization[7] and bone grafting scaffold.[8]

A variety of methods including sol-gel, spray pyrolysis, and surfactant templating have been employed to synthesize high surface area porous materials.[9–11] Polymer templating by hydrolysis and condensation of metal alkoxide on a polymer matrix to give porous metal oxides upon removal of polymer matrix has been one of the most common routes.[12,13] Also, condensing zirconia precursor on a polymer template to produce porous zirconia has been reported.[14] But, cost of starting materials and tedious procedures involved in the porous zirconia synthesis[15] limited widespread implementation.

Ram and coworkers[16] investigated the influence of precipitation pH, rate of addition of base, and heat treatment temperature on the speciation and crystal structure of zirconia formed. Their study showed that rapid base addition leads to monoclinic ZrO_2 whereas slow addition results in tetragonal ZrO_2 following heat treatment at 500°C. They also claimed that the type of zirconium salt as reactant coupled with the precipitation pH alter the crystal structure of the zirconia formed. In general, intermediate pH (i.e., ~7–10) results in monoclinic ZrO_2, while the tetragonal phase was observed at low and high pH conditions. It appears that the observations related to the rate of base addition and solution pH are coupled. The slow addition of base to a highly acidic solution always results in precipitation in low pH medium, whereas high rate of base addition will lead to locally higher pH values that might result in monoclinic zirconia. As the rate of base addition may also affect the primary particle size, it may also play a role in the structure of the zirconia formed after heat treatment.

Synthesis of mesoporous zirconia using polymeric templates has been reported previously.[17] Rezaei *et al.* precipitated zirconia over Pluronic P123 templates and reported surface area ranging from 25 to 130 m^2/g after calcination at 600°C depending on refluxing time and temperature. Higher refluxing temperature and time led to higher surface areas. However, specific surface area decreased progressively with the calcination temperature to about 75 m^2/g at 800°C, the highest temperature reported.

Zhou *et al.*[2] demonstrated the templation of titanium dioxide on agarose. Agarose is a polysaccharide widely used in biological studies such as electrophoresis or culture media. It can form a gel at a very low concentration, less than 6 wt%, and it is claimed to exhibit a two-step gelation mechanism. According to Zhou *et al.*, after dissolving in water around 90°C, agarose forms helices by hydrogen bonding upon cooling to about 60°C with a concomitant increase in viscosity. Further lowering the temperature to ambient leads to hydrogel formation during which 100–10 000 helices would bundle together to build a network of agarose fibers with a nanoscale diameter.[18–20]

In this article, a novel process for synthesis of mesoporous zirconia by *in situ* polymer templation employing low-cost agarose and zirconyl nitrate hydrate ($ZrO(NO_3)_2{\cdot}xH_2O$) is presented. In contrast with the previous study of agarose templation of titania by Zhou *et al.*, the synthesis procedure in this study employs only aqueous solvent during templation and utilized freeze-drying to remove the water. Freeze-drying is employed to avoid structural collapse of the agarose fiber network due to water evaporation. Taking advantage of the agarose gel formation, a uniform distribution of zirconium salt in the hydrogel network is realized. Precipitation of

P. Colombo—contributing editor

Manuscript No. 31552. Received June 01, 2012; approved July 25, 2012.
[†]Author to whom correspondence should be addressed. e-mail: makinc@iastate.edu

zirconia on (or within) the agarose gel is induced by the addition of ammonium hydroxide followed by freeze-drying the precipitate while maintaining the agarose template network structure. Pure zirconia was obtained after pyrolyzing agarose from the freeze-dried agarose/zirconia nanocomposite in air. Formation of high surface area zirconia replicating the hierarchical morphology of agarose gel with macro and mesopores is demonstrated.

II. Experimental Procedure

(1) Materials

Zirconyl(IV) nitrate hydrate, 99.50% $ZrO(NO_3)_2{\cdot}xH_2O$ (where $x \approx 2.5$ by TGA) was purchased from Acros Organics (Geel, Belgium) and agarose polymer with a gelation temperature of 36 ± 4°C from Fisher Scientific (Pittsburgh, PA). Ammonium hydroxide was reagent grade (assay 28.74%), also obtained from Fisher Scientific. All chemicals were used as received. For solvent, deionized water with a resistivity of about 18 Ohm/cm was used.

(2) Synthesis of Agarose/Zirconia Nanocomposite

A volume of 6 wt% agarose solution is prepared by adding 0.6 g agarose powder into 10 mL deionized water and heated in a water bath to about 90°C with vigorous stirring until a clear solution is obtained. Dissolution of agarose was complete within a couple of minutes and no significant water loss is noted. A 10 mL 1*M* zirconyl(IV) nitrate solution is obtained by dissolving 2.3 g zirconium nitrate precursor to 10 mL deionized water. For synthesis of zirconia nanocomposite, equal volumes of zirconyl nitrate and agarose solution are mixed at 60°C. The final solution is ~3 wt% agarose and 0.42*M* $ZrO(NO_3)_2$. The solution is stirred and brought to room temperature which is gelled within 10 min. The solid-like gel is sliced into cubes with about 0.5 cm × 0.5 cm × 0.5 cm in length and immersed into excess ammonium hydroxide (assay 25–28%) for 24 h to induce precipitation. The precipitate was rinsed with deionized water three times to remove ammonium nitrate and excess ammonium hydroxide. The sample is then quenched in liquid nitrogen and freeze-dried for 2 d to obtain agarose/zirconia nanocomposite.[21] Zirconia precipitation in the absence of agarose was also carried out as a benchmark for comparison.

(3) Characterization

Freeze-dried agarose/zirconia nanocomposite is heat treated at 300°C, 500°C, 700°C, and 900°C for 3 h in air to pyrolyze agarose, follow crystallization, and evolution of the microstructure. Thermal decomposition of pure agarose gel, agarose/zirconia nanocomposite, zirconia precipitated in the absence of agarose, was followed by thermogravimetric analysis (TGA-7; Perkin Elmer, Downers, Grove, IL). All samples were dried at 60°C for 48 h prior to TGA to remove excess water, hence, improve the accuracy of the data. Morphology of the agarose gel, nanocomposites as precipitated and after heat treatment was studied using SEM (JSM-5910LV; JEOL, Tokyo, Japan) and TEM (Tecnai F20; Phillips Corporation, Schaumburg, IL). The degree of templating and agarose/zirconia interaction was studied using Fourier-transform infrared spectrometry (FTIR; Bruker IFS-66V, Bruker Optics Inc., Billerica, MA) by pressing KBr pellets containing ~1% sample. All the NMR experiments were carried out on a Bruker Biospin DSX-400 spectrometer (Bruker-Biospin, Rheinstetten, Germany) with a resonance frequency of 400 MHz for ^1H and 100 MHz for ^{13}C. A 7-mm double resonance probe was used with a magic angle spinning (MAS) frequency of 6.5 kHz. The 90° pulse length was 4.5 μs for ^1H and 4 μs for ^{13}C. A 100 s recycle delay was used in direct-polarization ^{13}C NMR experiments. A contact time of 1 ms was employed in cross-polarization experiments. 60 kHz ^1H heteronuclear decoupling was used during ^{13}C detection. In addition to agarose/zirconia nanocomposites, a 4 wt% pure agarose gel was used as a reference to identify the changes caused by the presence of zirconia.

Surface area and pore size distribution were determined from Nitrogen adsorption isotherms (Autosorb-1; Quantachrome, Boynton Beach, FL) by applying BET and Barrett–Joyner–Halenda (BJH) methods for specific surface area and pore size distribution, respectively. Crystallization of the amorphous precipitate was followed by powder X-ray diffraction (Phillips X-pert X-Ray powder diffraction; Phillips Co., Schaumburg, IL). XRD patterns were obtained in the range $15 < 2\Theta < 80°$ with a step size of 0.03°.

III. Results and Discussion

Agarose/zirconia nanocomposite is obtained by incorporating hydrated zirconyl ion tetramer $[Zr_4(OH)_8(H_2O)_{16}]^{8+22}$ in solution containing agarose. It is believed that the agarose polymer chains self-assemble through hydrogen bonds to form a single fiber.[18–20] As zirconium ions are mixed with the agarose at the solution stage, the precipitation of zirconia is believed to take place within the agarose fibers.[2] As the precipitation occurs between the primary fibers and within the bundle of fibers leading to gelation of agarose, aggregation of primary zirconia precursor particles would be confined within the polymer network structure. Upon heating in air, agarose is pyrolyzed simultaneously with dehydroxylation and crystallization of zirconia precursor with increasing temperature. The original porous network structure formed by the agarose gel is mimicked in the morphology of zirconia.

(1) Pyrolysis of Nanocomposites

All samples were dried at 60°C for 24 h before TGA to remove the free water confined in the hydrogel network. All but ~2–3 wt% of free water is removed as evident from the mass loss observed below 200°C as shown in Fig. 1. It is interesting to note that the precipitate without the agarose shows nearly 18% mass loss over the same temperature range. Even if one corrects for the agarose content, the mass loss for the agarose/zirconia precursor nanocomposite due to water would be around 12%. Apparently, the precipitate formed with agarose template retain one-third less water than zirconia precipitated in the absence of template. At 200°C, a sharp mass loss is observed for unwashed sample due to decomposition of crystalline ammonium nitrate, NH_4NO_3, a byproduct of precipitation reaction.[23] When ammonium nitrate is removed by washing the gel sample (agarose/zirconia washed sample trace in Fig. 1), the sharp mass loss disappears as expected. Agarose decomposes stepwise, with mass losses occurring around 240°C–300°C and 440°C–500°C (see agarose gel plot in Fig. 1). Considering that the 20 wt% weight loss is due to dehydroxylation of zirconium hydroxide, the agarose content in agarose/zirconia composite should be 32 wt% or the weight ratio for agarose/ZrO_2 in the hybrid material is around 32/57 = 0.56 which is in excellent agreement with the starting agarose/ZrO_2 ratio of 0.58.

(2) Templation Mechanism

Interaction between the inorganic phase and the organic polymer template is studied by FTIR. Figure 2 shows IR spectra of agarose gel (a), agarose with zirconyl nitrate (b), and gel after precipitation (c). All three spectra exhibit some common features. For instance, they all have a broad peak around 3400 cm^{-1} and a relatively sharp peak at 1635 cm^{-1} which are attributed to vibration and bending modes of OH of water. Because the samples are exposed to the atmosphere, even freeze-dried and calcined samples exhibit these peaks.[24]

Sharp peak at 1380 cm^{-1} is absent in pure agarose sample (a), whereas it appears after addition of zirconyl nitrate (b), and after precipitation (c), is due to ν_3 frequency of NO_3^-. After precipitation, the reaction byproduct ammonium

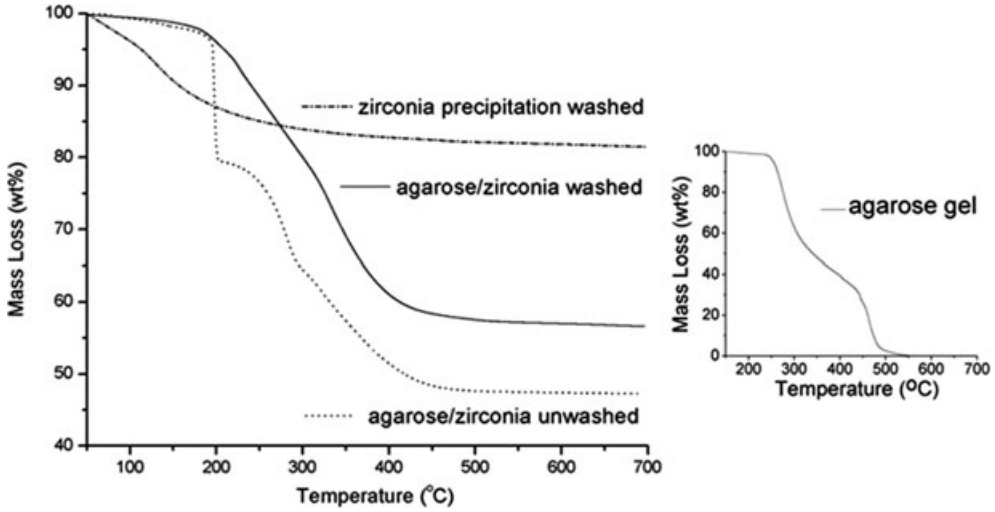

Fig. 1. Thermo gravimetric analysis of washed and unwashed agarose/zirconia nanocomposites. Also on the plot thermal decomposition of pure agarose gel, as well as zirconia precipitation (no agarose) are shown for comparison. Note that pure agarose decomposes over a temperature range up to 500°C, with two-step decomposition events one around 300°C the other around 450°C ,whereas zirconia precipitate shows a mass loss from room temperature to about 200°C which is attributed to evaporation of free water and deyhroxylation accounting for 15% mass loss.

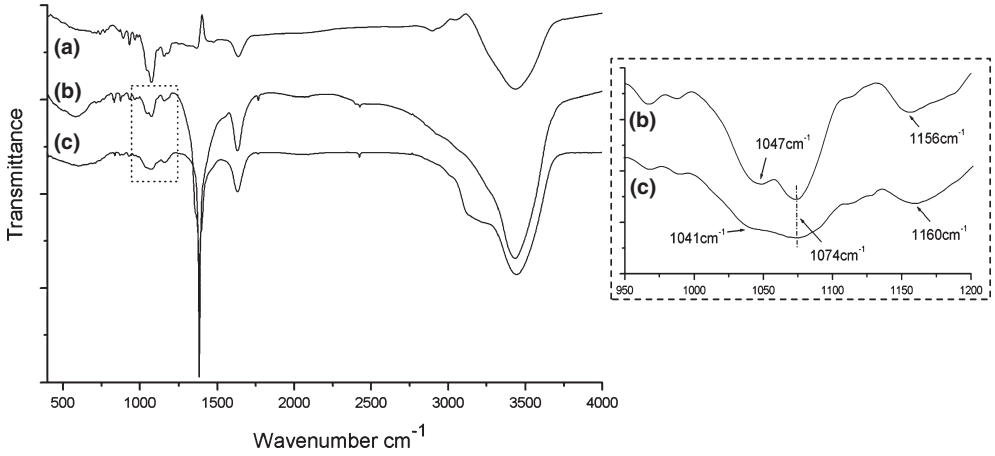

Fig. 2. FTIR spectral of samples (a) agarose gel, (b) agarose with zirconyl nitrate, (c) after precipitation. Note changes around 3200 cm^{-1} is due to N–H from NH_4^+. Also, precipitation of zirconia over agarose perturbs the absorption bands associated with C–O of primary and secondary alcohol groups.

nitrate fully crystallizes leading to a sharper and higher-intensity peak. Only samples after precipitation (Fig. 2) and freeze-drying (Fig. 3) show a shoulder at 3000–3200 cm^{-1} and is attributed to the overlap of $\nu_1 = 3040\ cm^{-1}$ and $\nu_3 = 3145 cm^{-1}$ N–H stretching frequencies of NH_4^+ ion.[24]

The peak at 1074 cm^{-1} is due to the glycosidic bond CH–O–CH in linear agarose polymer chain [see the molecular structure of agarose in Fig. 4(a)], and the peaks at 1147 and 1056 cm^{-1} are assigned to –C–O associated with the primary and secondary alcohol groups of agarose. After precipitation, these peaks broaden. The zirconia precipitate is either negatively or positively charged depending on pH. At very high pH, zirconia dissolves to form zirconium hydroxide anion. The following reaction was proposed at high pH[25,26]:

$$ZrO_2 + 2H_2O + OH^- \rightarrow Zr(OH)_5^-.$$

Under the experimental conditions used in this study, dissolution of zirconia is negligible. However, above its isoelectric point (H ≈ 4–5), zirconia exhibits negative charge and presumably associates with –OH groups of agarose. This association shifts the stretching frequency of –C–O as indicated in Fig. 2. The intensity of –C–O stretching in primary alcohol group (–CH_2OH) decreases compared with

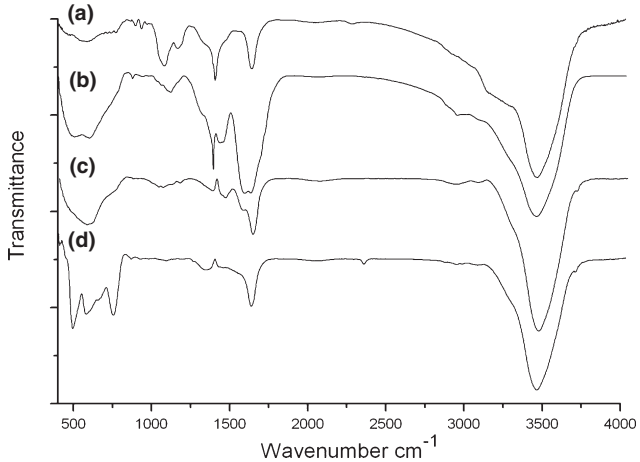

Fig. 3. FTIR spectra of samples (a) freeze-dried, and heated to (b) 200°C, (c) 300°C, (d) 500°C for 3 h.

secondary alcohol (–CHOH), which indicates a preference of inorganic species associating with CH_2OH over –CHOH groups and lends strong support to the polymer templating.

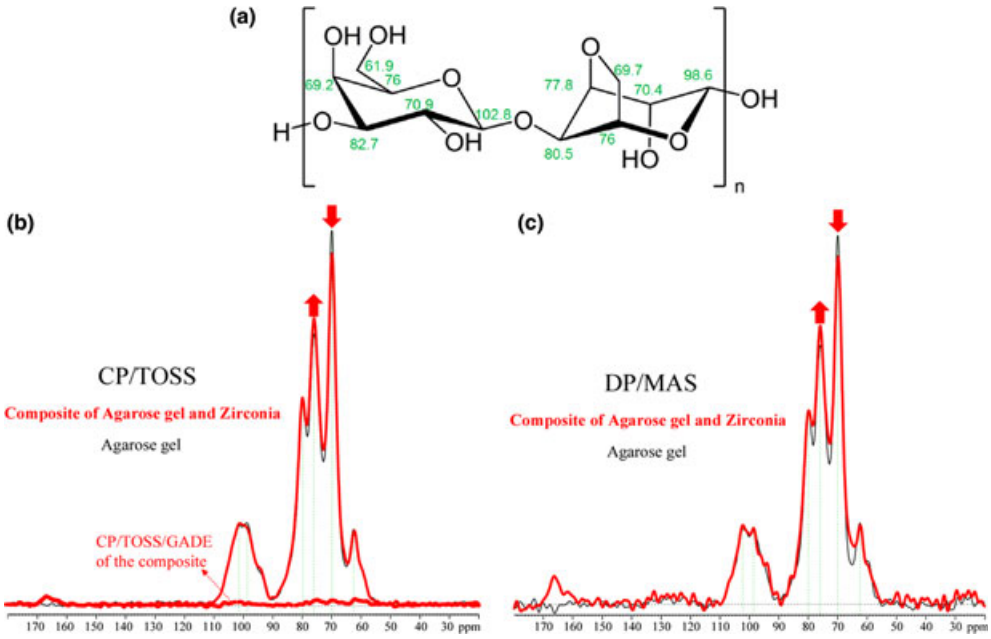

Fig. 4. ^{13}C NMR spectra of agarose gel and the composite of agarose and zirconia (4A0.5Z). (a) Structure of agarose and ^{13}C NMR chemical shifts from Brasch *et al.*[1] (b) ^{13}C cross-polarization with sideband suppression (CP/TOSS) NMR spectra of 4 wt% agarose gel (thin line) and the composite 4A0.5Z (thick line), along with the CP/TOSS spectrum after gated decoupling of the composite 4A0.5Z (the red thick line close to the baseline, labeled as CP/TOSS/GADE of the composite). (c) ^{13}C direct-polarization (DP) spectra of 4 wt% agarose gel (thin line) and the composite 4A0.5Z (thick line).

Besides, a series of small peaks from 800 to 1000 cm^{-1} due to the agarose galactopyranose units[27] broaden after NH_4OH addition. The broad peak around 500–800 cm^{-1} is due to Zr –O bond[28,29] of amorphous zirconia precipitate.

Removal of agarose by calcination of freeze-dried sample is illustrated in Fig. 3. Typical agarose polymer peaks of –C–O primary alcohol and tertiary alcohol stretching at 1147 and 1056 cm^{-1} gradually disappear with increasing temperature. In addition, successive small peaks at 880, 930, and 960 cm^{-1} attributed to agarose structure completely disappear after heating to 500°C (see Fig. 3). The shoulder at 3000–3200 cm^{-1} observed in freeze-dried sample, is also gone after heating to 200°C. The disappearance of the sharp peak at 1380 cm^{-1} of nitrate at 300°C is probably due to the stepwise decomposition of ammonium nitrate. Initial step of ammonium nitrate decomposition is by evaporation of ammonia as evidenced by the disappearance of shoulder at 3000–3200 cm^{-1}, although nitrate peaks at 1437 and 1575 cm^{-1},[24] disappear around 300°C.

The broad Zr–O peak around 500–800 cm^{-1} becomes more pronounced upon heating as zirconia becomes the major component following the removal of agarose and splits into three peaks, at 495, 580, 750 cm^{-1}, upon heating to 500°C. Indeed, as will be discussed later, the X-ray diffraction patterns indicate that tetragonal and monoclinic phases coexist for sample after heat treating at 500°C. Of the three Zr–O absorption peaks, 503 and 752 cm^{-1} were assigned to *m*-ZrO_2 whereas the one at 589 cm^{-1} was assigned to *t*-ZrO_2 in accordance with the bond lengths associated with the two crystallographic forms of ZrO_2.[28,29]

The freeze-dried agarose/zironia composite is studied by solid state ^{13}C NMR, together with the 3 wt% pure agarose gel used as a reference sample to identify the changes induced by the addition of zirconia. Literature values of ^{13}C NMR chemical shifts of agarose are marked (in ppm) in the structure shown in Fig. 4(a).[30] ^{13}C cross-polarization with sideband suppression (CP/TOSS) NMR spectra on agarose gel and the composite in Fig. 4(b) both exhibit five broad spectral bands, with CH_2OH resonating around 62 ppm, CH_nOH and CH_2OC at ca. 70 ppm, and others above 73 ppm. Compared with the spectrum of pure agarose gel, the spectrum of the composite shows a slightly decreased intensity of the spectral band centered around 70 ppm, which mainly corresponds to carbons bonded to OH, and accordingly increased intensity around 75 ppm. These spectral differences may be attributed to the conversion of C–O–H to C–O–Zr, which changes the involved ^{13}C chemical shifts from 70 to 75 ppm.[31] The direct-polarization (DP) ^{13}C spectra in Fig. 4(c) show the same trend, and the quantitative analysis of the intensity changes in these DP spectra indicates that ~7% of the C–O–H groups in agarose are converted to C–O–Zr. A broad peak at 166 ppm appears in the ^{13}C spectra of the composite, but is absent in the spectra of pure agarose gel. The much higher magnitude of this peak in the DP spectrum compared with the CP spectrum of the composite suggests that this carbon is not protonated, which is confirmed by the CP/TOSS spectrum after gated decoupling in Fig. 4(b) (the red line labeled as CP/TOSS/GADE of the composite), where the signal at 166 ppm is not dephased. This carbon is likely to be carbonate (CO_3^{2-}) generated from the incorporation of CO_2 from air during the synthesis process.[32]

The ^{13}C T_1 and T_2 relaxation times of pure agarose gel and the composite show no significant differences, suggesting the addition of zirconia in the agarose gel does not cause dynamic changes on the time scale of nanoseconds to microseconds.

(3) Structure

X-ray diffraction patterns of zirconia precipitates after freeze-drying with or without agarose remain amorphous up to 300°C as shown in Fig. 5. The small sharp line in the freeze-dried sample at $2\theta = 28.9°$ is attributed to the (111) plane of ammonium nitrate crystal. As discussed above, existence of ammonium nitrate in freeze-dried sample was indicated by an FTIR peak at $\nu_3 = 1380$ cm^{-1} for nitrate ion, and a shoulder at 3000–3200 cm^{-1} for ammonium ion. The peak at $2\theta = 28.9°$ disappears after heat treatment at 300°C proving that ammonium nitrate decomposition is completed by 300°C. At 400°C, weak diffraction peaks at $2\theta = 30°$, 50°, and 60°, belonging to (111), (112), and (211) planes of tetragonal phase were observed.[33] At 500°C, characteristic peaks at $2\theta = 28.3°$ for (−111) and 31.5° for (111) of monoclinic phase[33] appear indicating coexistence of tetragonal and

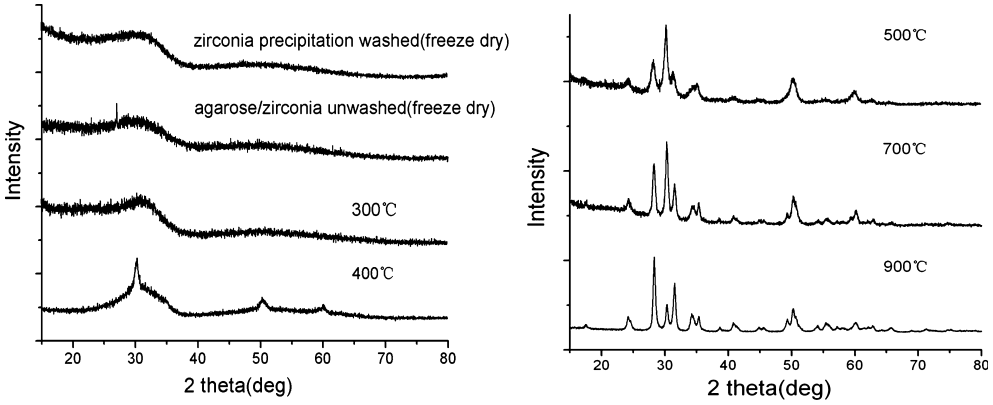

Fig. 5. XRD pattern of samples after heat treatment at indicated temperatures in air.

monoclinic phases. These two peaks increase, whereas the peak at 30.3° decrease with increasing temperature indicating gradual phase transformation from metastable tetragonal to stable monoclinic phase with increasing temperature.

The ratio of the two phases is related to the initial precipitation conditions.[16] The fraction of tetragonal phase zirconia, expressed using the following equation[34]:

$$F_t = (111)_t/[1.6(-111)_m + (111)_t]$$

and is plotted against the heat-treatment temperature (Fig. 6). Clearly as the heat-treatment temperature increases, the fraction of the tetragonal phase decreases from ~55% at 500°C to less than 20% in the 900°C heat treated sample.

Crystallite sizes are determined using Scherrer equation[35] and also shown in Fig. 6. From Fig. 6, it is evident that the crystallite sizes of both tetragonal and monoclinic phases increase with temperature as reported previously,[36] albeit that of the tetragonal is slower than that of the monoclinic phase. Crystal growth rates are complicated by the fact that during the same temperature tetragonal transforms to monoclinic phase.

(4) Morphology

Agarose hydrogel contains more than 90 wt% water. Upon drying, evaporation of water will draw gel fibers together and the original gel open network structure collapses.[19] To conserve the open porous structure for metal oxide formation, the hydrogel is freeze-dried. As showed in Fig. 7(a), highly porous fibrous network of the agarose gel is retained with a macropore size of about 0.1–0.5 μm. Figure 7(b) shows the open network structure of the hybrid material and resembles the macroporosity of pure agarose gel structure as illustrated in Fig. 7(a).

TGA results indicate that most of the agarose is removed by 300°C. Figure 8 shows the evolution of morphology of the zirconia with temperature as the nanocomposite was heated progressively to 900°C. As mentioned above, the organic phase is completely removed by 500°C. The heat treated material has a macropore size between 50 and 500 nm remarkably similar to that of pure agarose gel. Morphological features of pure zirconia after heat treatment are the same as that of freeze-dried agarose/zirconia hybrid and pure agarose gel. No visible structural collapse at this level occurs during heat treatment up to 900°C. Even after heating to 900°C, the fibrous network characteristic of pure agarose is still retained.

TEM micrographs illustrating the nanocrystalline, mesoporous structure of zirconia following heat treatment are shown in Fig. 9. The crystallite size ranges between 10 and 20 nm and agrees well with the XRD line-broadening estimates. TEM [Fig. 9(a)] also reveals that the pore diameter ranges from few nanometers to less than 100 nm. A closer examination of TEM images indicate that the darker area, is probably due to the overlap of zirconia fiber network structure, whereas edge of the sample [thin section shown in Fig. 9(b)] clearly reveals the porous structure. Crystallinity of the particles is evident from the moiré fringes. At higher magnifications, a bimodal pore size distribution is observed in agreement with the pore size distribution determined by adsorption isotherms: mesopores (<10 nm in diameter) surrounded by zirconia crystallites and larger pores surrounded by the zirconia agglomerates.

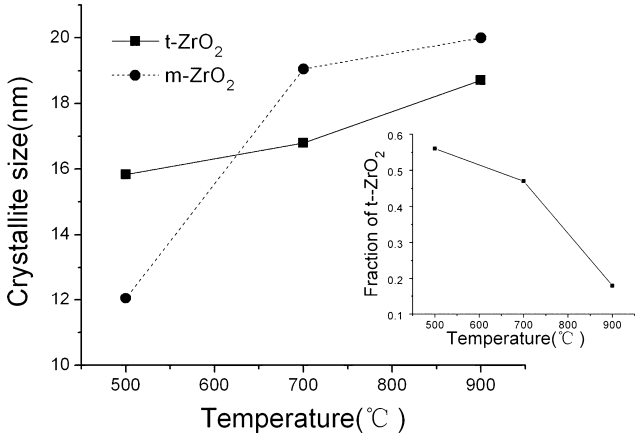

Fig. 6. Variation of crystallite sizes and phase fraction of *t*-zirconia with heat-treatment temperature.

(5) Mesoporosity

N_2-adsorption isotherms of all samples exhibit hysteresis loops indicative of mesoporous structure (Fig. 10). The sharp increase in adsorption at high relative pressures ($P/P_0 > 0.9$) is due to filling of larger pores with pore size, D, greater than 10 nm.[18–21] Specific surface area is calculated from the adsorption branch of the isotherm using the BET equation. The specific surface area of 3 wt% agarose gel after freeze-drying was determined to be 184 m^2/g. The adsorption isotherm for freeze-dried agarose/zirconia precursor hybrid material exhibits a similar hysteresis loop indicating that the porous structure of the agarose gel is preserved through the zirconia precipitation step. The specific surface area of the freeze-dried hybrid sample was determined to be 67 m^2/g which is still quite high but approximately one-third of that for freeze-dried agarose gel. There are two possible reasons for the observed reduction in specific surface. The first is due to the very definition of specific surface area. That is, as the mean density of the hybrid material is higher than the agarose because of higher zirconia

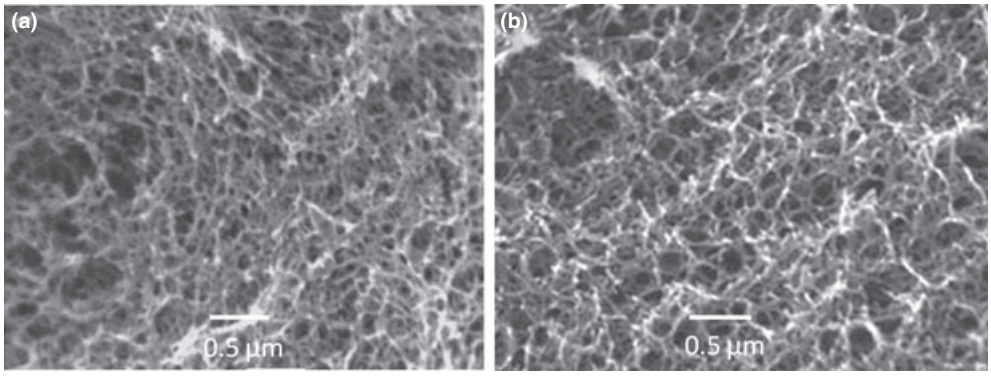

Fig. 7. SEM images of freeze-dried (a) 6 wt% agarose gel; (b) agarose/zirconia nanocomposite.

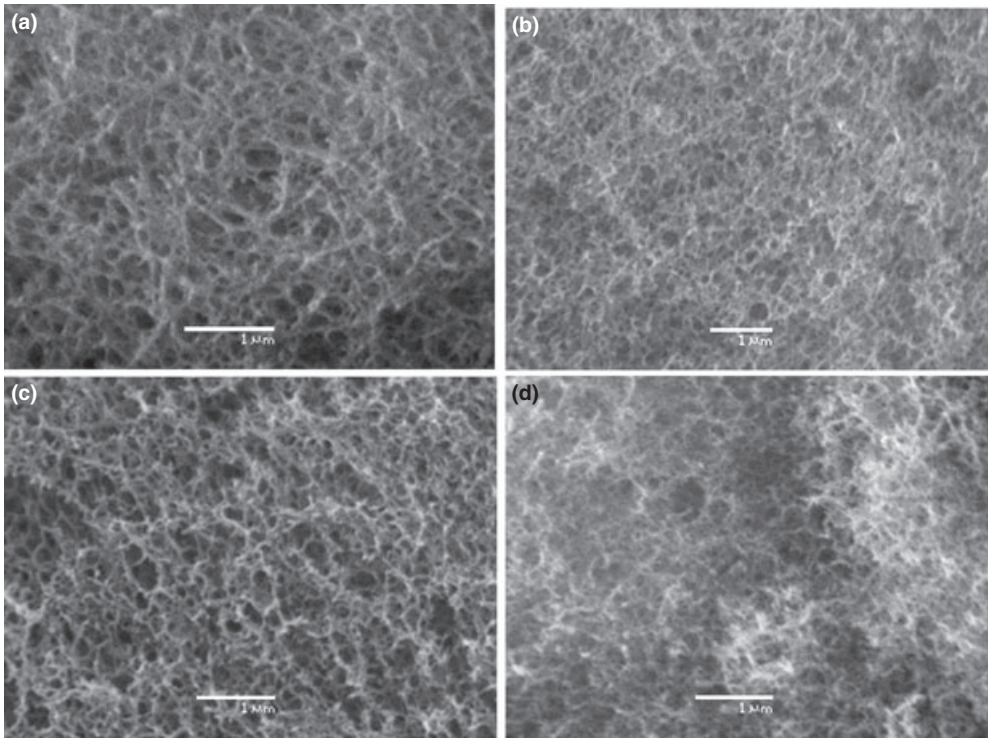

Fig. 8. SEM images of Zirconia samples after heating in air at: (a) 300°C, (b) 500°C, (c) 700°C, and (d) 900°C for 3 h

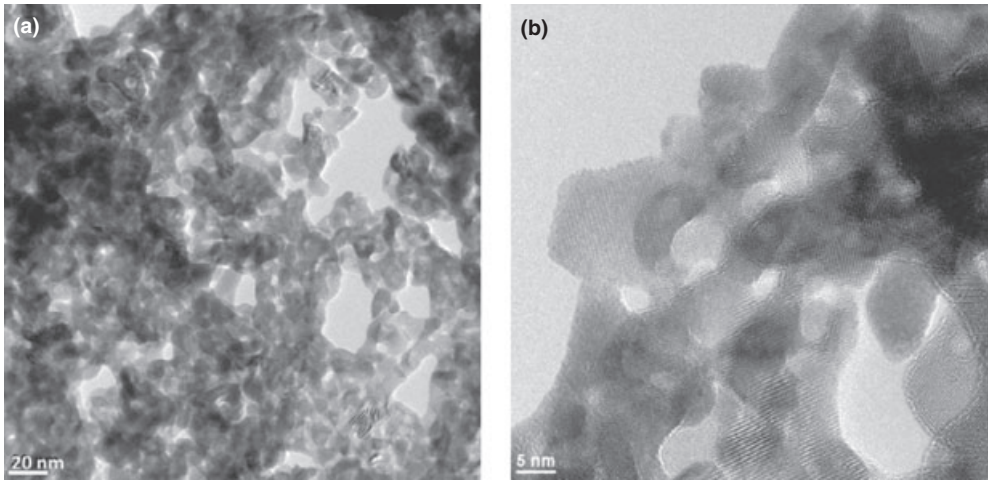

Fig. 9. TEM images of agarose/zirconia sample after heat treatment at 500°C (a) TEM, (b) HRTEM. Note the nanoparticles are on the order of 10–20 nm and show crystallinity in the HRTEM image.

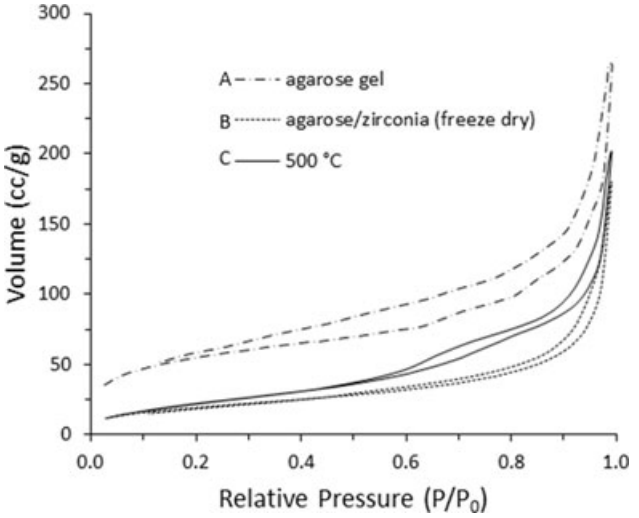

Fig. 10. N_2-adsorption/desorption isotherms. Although not shown on the plots, the initial point for each isotherm is origin. It should also be noted that the pure agarose gel shows a wider hysteresis loop than that of the freeze-dried agarose/zirconia composite. Finally, zirconia after agarose gel is removed, shows a bimodal size distribution one at $0.6 < P/P_0 < 0.8$, whereas the other is between $0.8 < P/P_0 < 1.0$ cm^3.

precursor density, there is less volume per gram of sample in the hybrid than in agarose gel alone. The second reason is probably due to reduction of agarose gel surface by zirconia precipitation, lowering the surface area.

Table I shows the change in surface areas after heating the sample for 3 h in air at the designated temperature. According to the TGA data (Fig. 1), by 300°C a little more than half of the agarose mass remains, and therefore the surface area at this temperature is still a combination of contributions from the agarose matrix and the templated zirconia. At 500°C the agarose template is completely removed leaving only the zirconia. The general appearance of the adsorption isotherm at this temperature indicates that zirconia fibers are strong enough to keep the original agarose/zirconia composite morphology even after removing the agarose template. The BET specific surface area of templated zirconia at this temperature is determined to be 86 m^2/g. However, increasing the temperature to 700°C and 900°C results in a significant decrease in surface area. As discussed earlier, the macroscale morphology in the SEM images (Fig. 8) did not appear to significantly change after heating. Therefore, the reduction in surface area must be due to structural collapse on the scale of mesopores.

The pore size distribution is determined from the desorption branch of the isotherms employing the classical BJH method. The pore size distribution of all samples covers the entire mesopores range (2–50 nm). These results are consistent with the SEM and TEM observations. Figure 11 shows the distribution in the smaller end of this range, highlighting the greater amount of pores in the <10 nm diameter range. The pure agarose gel has the greatest number of pores smaller than 5 nm of any sample, which is consistent with its large surface area. The loss of pores observed in the freeze-dried composite may be attributed to filling in by zirconia precursor precipitate. Mesopores with pore sizes between 2.5 and 5.5 nm are observed for all samples. A significant increase in mesopore volume is observed after heating the freeze-dried composite. By subtracting the freeze-dried pore volume from the heat treated sample, a sharp peak around 4–8 nm is obtained (see Fig. 11). If the appearance of the pores in this size range is attributable to removal of the agarose gel, one can claim that the structural scale of agarose fibers have the size scale of

Table I. Specific Surface Area Measured by Nitrogen Adsorption of Agarose and Agarose–Zirconia Composite Samples. Based on the TGA data (Fig. 1), the agarose should be completely removed by 500°C. Therefore, the surface area at this temperature and above represents the area of the templated zirconia only. It can be seen that the surface area of the templated zirconia decreases significantly with increasing temperature

Sample	Sample heat treatment (°C for 3 h)	Specific surface area (m^2/g)
Agarose	Freeze-dried	184
	Freeze-dried	67
	300	123
Agarose–zirconia composite	500	86
	700	28
	900	12

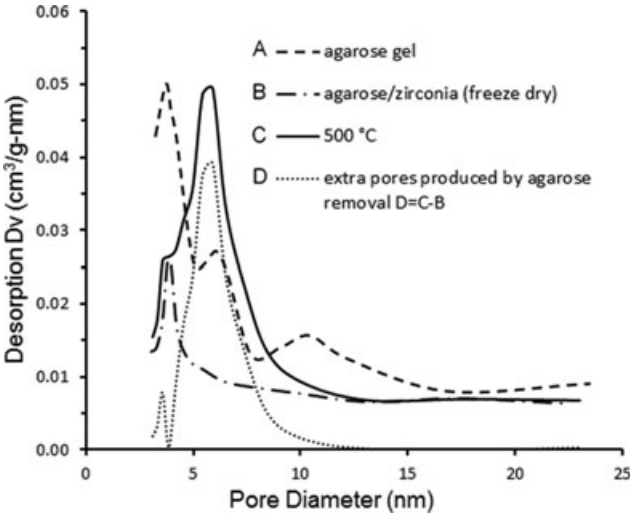

Fig. 11. The pore size distribution from the BJH desorption dV/dD plot. Subtracting the freeze-dried sample data from the 500°C heat treated sample reveals the pores created from agarose removal and an indication of feature size in agarose gel itself.

4–8 nm. This is in agreement with independent measurements of fiber diameter using diffusion, X-ray scattering, and gel chromatography.[37–39]

The isotherm for the heat treated sample shows a broader hysteresis loop extending to $P/P_0 < 0.6$ indicating presence of smaller pores. According to the Kelvin equation, the relative pressure range P/P_0 from 0.5 to 0.9 corresponds to mesopores with 2–10 nm in diameter.[40] This observation also confirms the nanoscale mixing of agarose with zirconia precursor. The appearance of mesopores may be attributed to either removal of the agarose gel or creation of mesoporosity during conversion of hydrous zirconia precursor to nanocrystalline zirconia. Provided that the agarose chains self-assemble to form helices, the nanoscale templating of zirconia with agarose helices will form the final hybrid fibers. The removal of agarose polymer with heat treatment results in numerous mesopores on the same size scale as agarose helices. Moreover, the dehydroxylation of zirconia precursor with heat treatment will also result in formation of mesopores.[41] A detailed analysis of heat treatment coupled with accurate knowledge of thermal decomposition of agarose and dehydroxylation of zirconia precursor is necessary for a better understanding of the mesopore evolution.

IV. Conclusions

Employing self-assembling agarose as a mineralization template, an agarose/zirconia hybrid material with a hierarchical pore structure is synthesized. Coulombic interaction between hydrous zirconia precipitate and hydroxyl groups of agarose provides the association force, although agarose gel appears to confine the solute to form zirconia that is uniformly distributed within the gel. After removal of agarose by pyrolysis, a mesoporous, crystalline zirconia is obtained. The specific surface area of agarose-zirconia composite before heating is found to be 67 m^2/g. After completely removing agarose by heating the sample to 500°C, the surface area of crystalline zirconia was determined to be 86 m^2/g, which reduced with increasing temperature down to 13 m^2/g above 900°C. Due to agarose removal and dehydroxylation of zirconia precipitate, a sharp increase in mesopore volume in the 4–8 nm size range is observed. The zirconia after heat treatment at 500°C shows a duplex structure consisting of 10–20 nm primary nanoparticles agglomerated to form a larger network structure similar to that of the templating agarose gel.

Acknowledgment

The work is supported by the U.S. Department of Energy under contract number DE-AC02-07CH11358.

References

[1]G. L. Drisko, V. Luca, E. Sizgek, N. Scales, and R. A. Caruso, "Template Synthesis and Adsorption Properties of Hierarchically Porous Zirconium Titanium Oxides," *Langmuir*, **25** [9] 5286–93 (2009).

[2]J. Zhou, M. Zhou, and R. A. Caruso, "Agarose Template for the Fabrication of Macroporous Metal Oxide Structures," *Langmuir*, **22** [7] 3332–6 (2006).

[3]J. H. Schattka, E. H.-M. Wong, M. Antonietti, and R. A. Caruso, "Sol-Gel Templating of Membranes to Form Thick, Porous Titania, Titania/Zirconia and Titania/Silica Films," *J. Mater. Chem.*, **16** [15] 1414–20 (2006).

[4]K. Kordesch and G. Simader, *Fuel Cells and Their Applications*. Wiley-VCH Publishers, New York, 1996.

[5]K. Tanabe and T. Yamaguchi, "Acid-Base Bifunctional Catalysis by ZrO_2 and its Mixed Oxides," *Catal. Today*, **20** [2] 185–98 (1994).

[6]T. V. Thamaraiselvi and S. Rajeswari, "Biological Evaluation of Bioceramic Materials – A Review," *Trends Biomater. Artif. Organs.*, **18** [1] 9–17 (2004).

[7]M. Huckel, *et al*., "Porous Zirconia: A New Support Material for Enzyme Immobilization," *J. Biochem. Biophys. Methods*, **31** [3–4] 165–79 (1996).

[8]H. W. Kim, "Porous ZrO_2 Bone Scaffold Coated with Hydroxyapatite with Fluorapatite Intermediate Layer," *Biomaterials*, **24**, 3277–84 (2003).

[9]C. Perego and P. L. Villa, eds. "The Catalytic Process from Laboratory to the Industrial Plant"; p. 293 in *Proceedings of the 3rd Seminar on Catalysis*, Edited by D. Sanfiljppo. Italian Chemical Society, Rimini, Italy, 1994.

[10]M. L. Occellia, S. Biza, A. Aurouxb, and G. J. Rayc, "Effects of the Nature of the Aluminum Source on the Acidic Properties of Some Mesostructured Materials," *Microporous Mesoporous Mater.*, **26** [1–3] 193–213 (1998).

[11]W. R. Moser, *Advanced Catalysts and Nanostructured Materials: Modern Synthetic Methods*. Academic Press, San Diego, CA, 1996, xxvi, p. 592

[12]A. Vantomme, A. Leonard, Z. Y. Yan, and B. L. Su, "Hierarchically Nanostructured Porous Functional Ceramics"; pp. 1933–8 in *High-Performance Ceramics IV*, Pts 1–3, Edited by W. Pan and J. H. Gong. Trans Tech Publications Ltd, Stafa-Zurich, 2007.

[13]H. Zhang, G. C. Hardy, Y. Z. Khimyak, M. J. Rosseinsky, and A. I. Cooper, "Synthesis of Hierarchically Porous Silica and Metal Oxide Beads Using Emulsion-Templated Polymer Scaffozds." *Chem. Mater.*, **16** [22] 4245–56 (2004).

[14]R. N. Das, S. Nad, and P. Pramanik, "Nanocrystalline Yttria-Stabilized Zirconia Fibers from Plant Fibers and Their Polymer Composites," *J. Am. Ceram. Soc.*, **91** [3] 1034–6 (2008).

[15]G. K. Chuah, "An Investigation into the Preparation of High Surface Area Zirconia," *Catal. Today*, **49** [1–3] 131–9 (1999).

[16]R. Srinivasana, M. B. Harrisa, S. F. Simpsona, R. J. De Angelisa, and B. H. Davis, "Zirconium Oxide Crystal Phase: The Role of the pH and Time to Attain the Final pH for Precipitation of the Hydrous Oxide," *J. Mater. Res.*, **3** [4] 787–97 (1988).

[17]M. Rezaei, S. M. Alavi, S. Sahebdelfar, and Z.-F. Yan, "Effect of Process Parameters on the Synthesis of Mesoporous Nanocrystalline Zirconia with Triblock Copolymer as Template," *J. Porous Mater.*, **15** [2] 171–9 (2008).

[18]S. Arnott, A. Fulmer, and W. E. Scott, "Agarose Double Helix and its Function in Agarose Gel Structure," *J. Mol. Biol.*, **90** [2] 269–84 (1974).

[19]D. A. Rees and E. J. Welsh, "Secondary and Tertiary Structure of Polysaccharides in Solutions and Gels," *Angew. Chem. Int. Ed.*, **16** [4] 214–23 (1977).

[20]H. Itagaki, H. Fukiishi, T. Imai, and M. Watase, "Molecular Structure of Agarose Chains in Thermoreversible Hydrogels Revealed by Means of a Fluorescent Probe Technique,"
J. Polym. Sci. Part B Polym. Phys., **43** [6] 680–8 (2005).

[21]E. Fernándeza, C. Mijangosa, J. M. Guenetb, M. Teresa Cuberesc, and D. Lópeza, "New Hydrogels Based on the Interpenetration of Physical Gels of Agarose and Chemical Gels of Polyacrylamide," *Eur. Polym. J.*, **45** [3] 932–9 (2009).

[22]M. A. Blesa, A. J. G. Maroto, S. I. Passaggio, N. E. Figliolia, and G. Rigotti, "Hydrous Zirconium Dioxide: Interfacial Properties, the Formation of Monodisperse Spherical Particles, and its Crystallization at High Temperatures," *J. Mater. Sci.*, **20** [12] 4601–9 (1985).

[23]P. Patnaik, *Handbook of Inorganic Chemicals*. McGraw-Hill, New York, 2002.

[24]M. N. Rahaman, *Ceramic Processing and Sintering*. *Materials Engineering*. M. Dekker. Inc., New York, 2003, p. 875.

[25]I. A. Sheka and T. V. Pevzner, "Solubility of Zirconium and Hafnium Hydroxides in Sodium Hydroxide Solution," *Zh. Neorg. Khim.*, **5** [10] 2311–4 (1960).

[26]S. Roy, "Nanocrystalline Undoped Tetragonal and Cubic Zirconia Synthesized Using Poly-Acrylamide as Gel and Matrix," *J. Sol-Gel. Sci. Technol.*, **44**, 227–33 (2007).

[27]H. T. Rijnten, "Formation, preparation and properties of hydrous zirconia"; pp. 315–72 in *Physical Chemistry and Aspects of Adsorbent and Catalysts*, Edited by B. G. Linsen. Academic, New York, 1970.

[28]V. Sánchez Escribano, C. del Hoyo Martínez, E. Fernández López, J. M. Gallardo Amores, and G. Busca, "Characterization of a Ceria-Zirconia-Supported Cu Oxides Catalyst: An FT-IR Study on the Catalytic Oxidation of Propylene," *Catal. Commun.*, **10** [6] 861–4 (2009).

[29]A. A. M. Ali and M. I. Zaki, "Thermal and Spectroscopic Studies of Polymorphic Transitions of Zirconia During Calcination of Sulfated and Phosphated Zr(OH)(4) Precursors of Solid Acid Catalysts," *Thermochim. Acta*, **336** [1–2] 17–25 (1999).

[30]D. J. Brasch, C. T. Chuah, and L. D. Melton, "A C-13 Nmr-Study of Some Agar-Related Polysaccharides from New-Zealand Seaweeds," *Aust. J. Chem.*, **34** [5] 1095–105 (1981).

[31]V. Salinier, G. P. Niccolai, V. Dufaud, and J. M. Basset, "Silica-Supported Zirconium Complexes and Their Polyoligosilsesquioxane Analogues in the Transesterification of Acrylates: Part 2. Activity, Recycling and Regeneration," *Adv. Synth. Catal.*, **351** [13] 2168–77 (2009).

[32]Y. Yusufoglua, Y. Hu, M. Kanapathipillaia, M. Kramera, Y. E. Kalaya, P. Thiyagarajana, M. Akinc, K. Schmidt-Rohra, and S. Mallapragada, "Bioinspired Synthesis of Self-Assembled Calcium Phosphate Nanocomposites Using Block Copolymer-Peptide Conjugates,"
J. Mater. Res., **23** [12] 3196–212 (2008).

[33]The International Centre for Diffraction Data. 2008, ICDD DDView + 4.8.0.0 PDF-4 RDB 4.0804, Newtown Square, PA.

[34]D. L. Porter and A. H. Heuer, "Microstructural Development in Mgo-Partially Stabilized Zirconia (MG-PSZ)," *J. Am. Ceram. Soc.*, **62** [5–6] 298–305 (1979).

[35]B. D. Cullity and S. R. Stock, *Elements of X-Ray Diffraction*, 3rd Edition. Prentice Hall, 2001.

[36]P. Kountouros and G. Petzow, "Defect chemistry, phase stability and properties of zirconia polycrystals"; pp. 30–48 in *Science and Technology of Zirconia V*, Edited by S.P.S. Badwal, M.J. Bannister, and R.H.J. Hannink. Technomic Publishing Company Inc, Lancaster, PA, 1993.

[37]A.e.a. Pluen, "Diffusion of Macromolecules in Agarose Gels: Comparison of Linear and Globular Configurations," *Biophys. J .*, **77**, 542–52 (1999).

[38]M. Djabourov, A. H. Clark, D. W. Rowlands, and S. B. Ross-Murphy, "Small-Angle X-ray Scattering Characterization of Agarose Sols and Gels," *Macromolecules*, **22**, 180–8 (1989).

[39]T. C. Laurent, "Determination of the Structure of Agarosegels by Gel Chromatography," *Biochim. Biophys. Acta*, **136** [2] 199–205 (1966).

[40]S. Gregg and K. Sing, *Adsorption, Surface Area and Porosity*, 2nd edition. Academic Press, London, New York, 1982.

[41]P. Trens, M. J. Hudson, and R. Denoyel, "Formation of Mesoporous, Zirconium(IV) Oxides of Controlled Surface Areas," *J. Mater. Chem.*, **8** [9] 2147–52 (1998). □